

Damage production in GaAs and GaAsN induced by light and heavy ions

C. Björkas,^{a)} K. Nordlund, K. Arstila, and J. Keinonen

Accelerator Laboratory, University of Helsinki, P.O. Box 43, Helsinki FIN-00014, Finland

V. D. S. Dhaka

Institute of Materials Chemistry, Tampere University of Technology, P.O. Box 692, 33101 Tampere, Finland

M. Pessa

Optoelectronics Research Centre, Tampere University of Technology, P.O. Box 692, 33101 Tampere, Finland

(Received 13 January 2006; accepted 17 July 2006; published online 12 September 2006)

Ion irradiation causes damage in semiconductor crystal structures and affects charge carrier dynamics. We have studied the damage production by high-energy (100 keV–10 MeV) H, He, Ne, and Ni ions in GaAs and GaAs₉₀N₁₀ using molecular dynamics computer simulations. We find that the heavier Ne and Ni ions produce a larger fraction of damage in large clusters than H and He. These large clusters are either in the form of amorphous zones or (after room-temperature aging or high-temperature annealing) in the form of vacancy and antisite clusters. The total damage production in GaAs and GaAs₉₀N₁₀ is found to be practically the same for all the ions. A clearly smaller fraction of the damage in GaAs₉₀N₁₀ compared to GaAs is in large clusters, however. Our results indicate that experimentally observed differences in charge carrier lifetimes between light and heavy ion irradiations, and before and after annealing, can be understood in terms of the large defect clusters. An increasing amount of damage in large clusters decreases the carrier decay time.

© 2006 American Institute of Physics. [DOI: 10.1063/1.2336306]

I. INTRODUCTION

Semiconductors based on gallium arsenide are of great interest as materials for their unique properties and a wide range of possible device applications.¹ In particular, semiconductor heterostructures based on InGaAsN compounds with varying In and N contents are widely used as active regions in semiconductor saturable absorber mirrors (SESAMs) and quantum well lasers operating at 1.3–1.55 μm wavelength range.^{2–6} Recently, it has been shown that heavy ion irradiation can be used to strongly modify the charge carrier dynamics in such GaAs based semiconductor devices.^{2,7–11} Reductions in the charge carrier lifetime of up to three orders of magnitude have been reported,^{10,11} making ion irradiation a promising method for manufacturing very fast SESAMs.⁷

The effects of ion irradiation on carrier dynamics are known to be related to crystal defects, but which defect types, in particular, affect the dynamics is not fully understood. Previous studies of the effect^{8–10} have attributed the reduction to large defect clusters, based on the observation that heavy ions are most efficient in facilitating the effect and on transmission electron microscopy (TEM) experiments where large defect clusters are visible.

Until recently, there were, however, no systematic studies of what ion mass and energy ranges, and correspondingly what defect cluster sizes, cause the desired effects. Moreover, the attribution of the carrier lifetimes to defect clusters visible in a TEM is complicated by the experimental observation that such clusters anneal away with time even at room temperature.¹² Recently, Dhaka *et al.* have systematically ex-

amined the effects different ions, doses, and ion energies have on the charge carrier dynamics in GaAs-based semiconductor structures.^{11,13,14} The results clearly show that different ions in irradiation at kinetic energies that produce the same nuclear energy deposition in the active region yield very different carrier decay times. This is illustrated in Fig. 1, with data reproduced from Ref. 11. This shows that the decay time does not only depend on the total amount of dam-

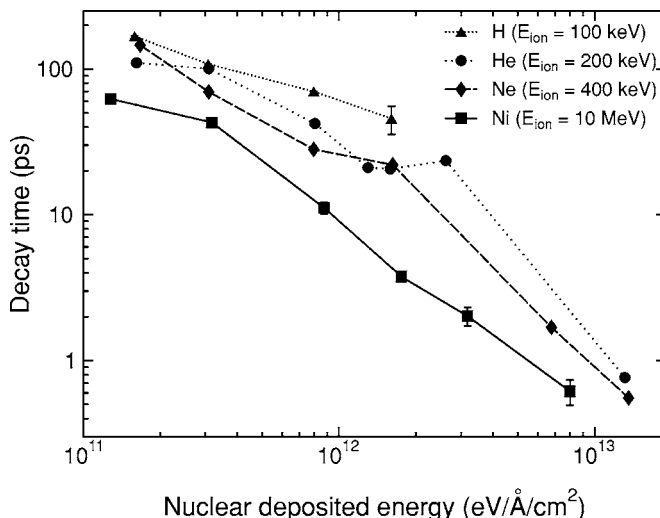


FIG. 1. Charge carrier decay time in InGaAs/GaAs quantum wells (QWs) as a function of nuclear deposited energy. The studied samples consisted of five compressively strained QWs made of 6-nm-thick In_{0.29}Ga_{0.71}As/17 nm GaAs heterostructures deposited onto a 200 nm GaAs buffer in a GaAs (001) substrate and capped with a thin GaAs layer. Time-resolved photoluminescence (TRPL) was measured using a femtosecond upconversion method, as described in Ref. 38. The deposited energies were calculated with the SRIM-2003 code (Ref. 39). Additional details of the experiment can be found in Ref. 11.

^{a)}Electronic mail: bjorkas@acclab.helsinki.fi

age, but also on its type, and is thus well in line with the previous interpretation that defect clusters are responsible for the damage.

To obtain additional atom-level understanding of what kind of defect clusters are related to the charge carrier lifetimes, in the current paper we use atomistic computer simulations of the ion irradiation process to predict the defect cluster sizes obtained for the same irradiation conditions as those presented in Ref. 11. Using a combination of molecular dynamics range calculations¹⁵ and calculations of damage induced by recoils¹⁶ we can predict the damage production induced by keV and MeV ion implantations.^{17,18} Comparison of these results with the experimental ones on carrier lifetime reduction during irradiation, room-temperature aging, and high-temperature annealing enable us to show that the behavior of large (initially more than 70 disordered atoms) clusters can indeed explain the experimental results.

II. METHOD

We chose to study both GaAs and GaAs_{1-y}N_y (with low N contents *y*) since these materials are of great current interest for optoelectronic applications.^{2,7} It is interesting to consider the presence of N on the damage production because of the large mass difference of N and As and the huge difference in damage production between stoichiometric GaAs and GaN.¹⁹⁻²¹ In contrast, we do not consider InGaAs since the relative mass difference between In and Ga/As is clearly less than that of N, making it unlikely that In affects the nature of damage qualitatively. In a previous work we did consider cascades in both InAs and GaAs, but did not observe any major differences between the overall cascade structure in the two materials.²²

Because of the long (order of microns) penetration depths of the ions, it is impossible to simulate the damage production of the 0.1–10 MeV ions in a single molecular dynamics (MD) simulation. Hence we first use MD range calculations¹⁵ to obtain the recoil spectra of the high-energy ions (with initial kinetic energy E_{ion}) in the depth region of interest, and then MD simulations of the full development of collision cascades to obtain the damage production by individual recoils (with initial kinetic energy E_{rec}). By integrating the two, we obtain the damage production of the ions in the active semiconductor layers.

A. MDRANGE calculations

Ion irradiation simulations on GaAs and GaAs₉₀N₁₀ (hereafter referred to as GaAsN) were performed using the MDRANGE code.²³ This code makes use of an approximation in which the interaction between a recoil atom and lattice atoms is taken into account but interactions between lattice atoms are neglected, due to the fact that in the keV energy regime interactions between the recoil atom and its nearest neighbors are much stronger than interactions between other lattice atoms.

The universal Ziegler-Biersack-Littmark (ZBL) repulsive potential was used, and the ZBL96 electronic stopping power^{24,25} were included in the MDRANGE calculations. 100 keV H ions, 200 keV He ions, 400 keV Ne ions, and

10 MeV Ni ions were allowed to irradiate bulk GaAs and GaAsN at incident directions 0° and 7° off the [100] crystal direction normal to the sample surface, thereby allowing calculations of ion channeling in a random rotation angle around the [100] axis. 10 000 recoil events were computed for each ion. The deposited energy and damage production was calculated between the depths of 80 and 200 nm from the sample surface, corresponding to typical depths of the active region.^{2,7,11}

The deposited nuclear energy was calculated to estimate the damage production. Statistics on the number of primary recoils of energy E_{rec} produced in the active region per incoming ion of energy E_{ion} , i.e., the integrated primary recoil spectra $n_t(E_{\text{rec}})dE_{\text{rec}}$ (*t* represents the atom type, Ga, As, or N), were used to estimate primary damage. The spectra were used to calculate the total damage N_{tot} produced in the implantation according to

$$N_{\text{tot}}^D = \sum_{t=1}^{N_t} \int_0^{\infty} N_t^D(E_{\text{rec}})n_t(E_{\text{rec}})dE_{\text{rec}}. \quad (1)$$

Here, N_t is the number of types of atoms (Ga, As, and N), N_t^D describes the number of defects produced for a given self-recoil process, and *D* denotes some specific type of damage. The N_t^D data are presented in Sec. III B. Earlier studies¹⁸ showed that the damage produced by As self-recoil was essentially the same as that produced by Ga self-recoil, i.e., $N_{\text{As}}^D = N_{\text{Ga}}^D$. The function N_t^D was fitted to the simulation data for total damage and for damage in small and large clusters. The fitted curves were of a combined logarithmic and linear form, $N_t^D = a \log(bx) + cx + d$, while a linear approximation was sufficiently accurate for large clusters. The recoils were assumed to be produced far from each other so that the resulting cascades are nonoverlapping.

B. Interatomic potentials

In the self-recoil calculations, the interactions between lattice atoms could not be ignored for obvious reasons. The interatomic potentials used for Ga–Ga, As–Ga, and As–As in GaAs and Ga–N in GaAsN are based on the Tersoff formalism and modified and developed by Albe *et al.*²⁶ The parameters used for the As–As potential were the same as those used for the As–N potential. This approximation should be a reasonable choice because As–N bonds may only exist in small clusters and amorphous pockets and because we did not aim at studying them in detail.

C. MD simulations

To obtain N_t^D , collision cascade simulations in bulk GaAs and GaAsN were made with the MD code PARCAS.²⁷ For GaAs with recoil atoms of energies up to 400 eV the simulation cell consisted of 11 unit cells; for the 1–10 keV energy range the simulation cell consisted of 15–33 unit cells. For GaAsN the simulations at recoil energies of 2 keV needed a slightly larger cell than what was used for GaAs because of the longer range of the light nitrogen atoms: 22 unit cells for 2 keV and 38 for 5 keV. Periodic boundary conditions²⁸ were used at the simulation cell borders in all

three dimensions. The simulation cells were initially thermally equilibrated at 300 K for 10 ps. Berendsen pressure control²⁹ was used to keep the cell at zero pressure during this initial simulation.

The thermally equilibrated simulation cell was then used for the recoil calculations. For GaAs a recoil energy was given to an As atom near the center of the cell. For GaAsN, a recoil energy was given to both As and N (collision cascades with gallium acting as a recoil atom would result in the same damage as arsenic would do). In these simulations, Berendsen temperature control²⁹ with a time constant of 100 fs was used to scale the temperature at the cell boundary, the thickness of which was taken to be one lattice constant. No pressure control was used during the cascade simulations.

The movement of the atoms was monitored in such a way that if the energy of any atom in the border region exceeded 10 eV, the simulation was stopped and then restarted with an initial recoil position placed farther away from the border. After 8 ps the temperature was slowly quenched to 0 K at a rate of 0.01 K/fs to enable defect analysis unaffected by thermal vibrations. The ZBL electronic stopping model²⁴ was applied to atoms with a kinetic energy above 5 eV. 5 eV is chosen since this energy is somewhat above the cohesive energy of the lattice—at lower energies the concept of electronic stopping is not meaningful as the ion cannot travel in the lattice. Tests showed that the results are not sensitive to the exact value of this energy limit.

D. Defect analysis

Two different types of defect analyses were performed. First, for GaAs and GaAsN, a Wigner-Seitz (WS) cell,³⁰ centered on each lattice site, was used to find vacancies and interstitial atoms. A lattice site with an empty Wigner-Seitz cell was labeled a vacancy, and a cell with multiple atoms an interstitial [we use the conventional crystallographic definition of a Wigner-Seitz cell (Ref. 30)]. Second, for GaAs, the potential energy (E_p) analysis was performed. In the latter case an atom with E_p more than 0.2 eV above potential energy equilibrium was regarded as a structural defect.

The defects were divided into clusters of different sizes. For vacancies and interstitial defects we carried out a cluster connectivity analysis, i.e., calculated the distance from all defects to all others. All defects that were within a fixed cutoff radius from each other were interpreted to be part of the same defect cluster. The cut-off radius was chosen to be one lattice constant (0.565 nm for GaAs and 0.552 nm for GaAsN). Visual analysis of the defects produced in individual cases was used to choose the potential energy analysis cluster connectivity cutoff radii such that the WS-defect clusters and potential defect clusters corresponded well to each other in spatial extension. For the E_p analysis this procedure gave a cutoff radius of 0.392 nm.

Point defects, and small and large clusters were distinguished from each other such that small clusters contained 2–10 WS defects or 10–70 E_p defects. These limits were found to correspond well to each other based on visual

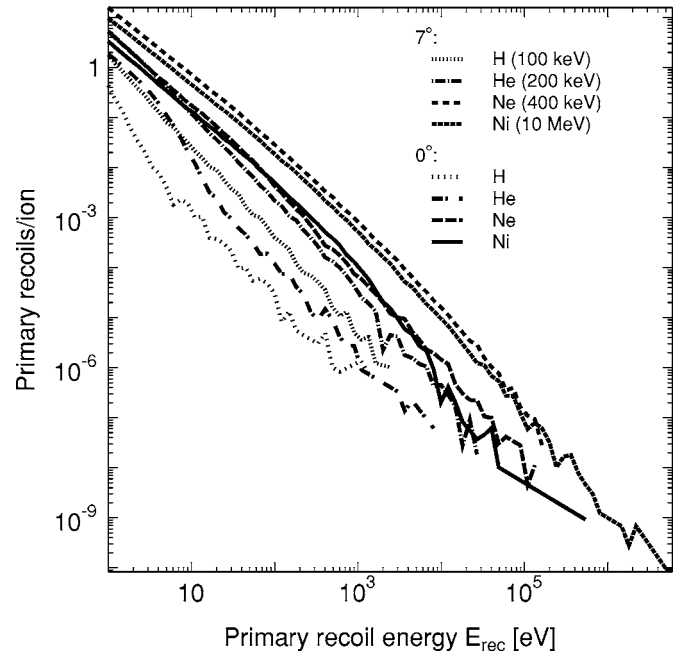


FIG. 2. The average number of primary As recoils for ion implantations in GaAs. Data are shown for an irradiation angle of 7° and for an angle of 0° off the [100] crystal direction.

analysis. A single Ga atom on an As site, or an As or N atom on a Ga site, was defined as an antisite defect.

III. RESULTS

A. Recoil spectra

The recoil spectra $n_i(E_{\text{rec}})dE_{\text{rec}}$ are illustrated in Figs. 2 and 3. Figure 2 shows that the number of primary As recoils produced per incoming ion depends on the irradiation direc-

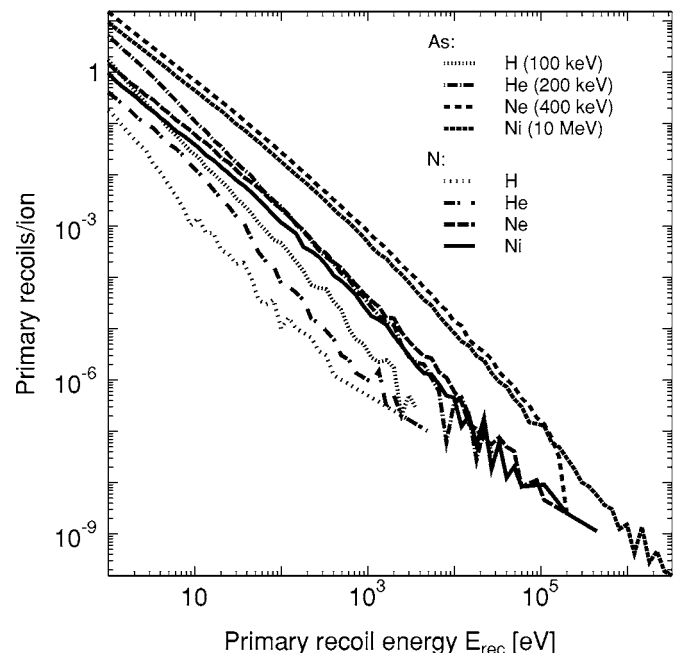


FIG. 3. The average number of primary recoils for ion implantations in GaAs₉₀N₁₀ using an irradiation angle of 7° off the [100] crystal direction. Both the number of As and N primary recoils are shown.

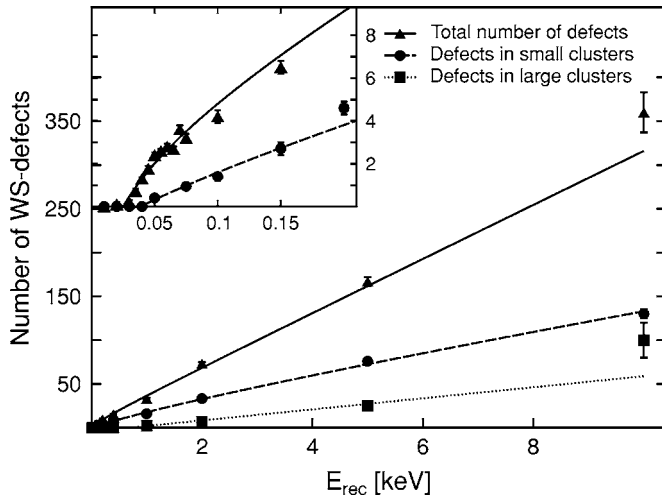


FIG. 4. WS defects produced by As recoils in GaAs. Small clusters are clusters containing two to ten WS defects.

tion. We used a threshold energy of 1 eV for primary recoils in the recoil spectra $n_i(E)$, which is well below the smallest possible energy which can cause damage production. Since the fitted damage production curves N_i^D all had an energy threshold E_i clearly larger than 1 eV, this lower limit does not affect the final damage production values N_{tot}^D obtained using Eq. (1).

At 7° , there are more primary recoils than at 0° , due to an ion channeling phenomenon, which is more pronounced for the 0° direction. The same channeling effect is seen for the total damage production in Table IV. Figure 2 shows that up to a certain energy, Ne produces more primary recoils than do energetic Ni ions. The Ni ions can produce, albeit seldom, primary recoils with a recoil energy E_{rec} as high as 6 MeV. The maximum deposited energy depends on the atomic mass, as shown in Fig. 2. A comparison between the recoil spectra for N and As in GaAsN (Fig. 3) indicates that the energy of a recoil atom is received by As rather than N.

B. Ion collision cascade results

The results of the cascade simulations are shown in Figs. 4–6. The fitted lines are asymptotically linear and the error bars show the standard error of the average. The insets show the damage production at low E_{rec} .

Low-energy simulations ($E_{\text{rec}} < 400$ eV) provided threshold energies for the formation of point defects, small clusters, and large clusters. According to Fig. 4, these energies are about 25, 50, and 650 eV, respectively, for the cascades in GaAs. At 10 keV recoils, almost every large cluster contained 50 or more defects. The largest cluster produced was a cluster of as many as 281 vacancies.

The largest cluster in GaAsN was a cluster of 32 vacancies. This was produced with a 2 keV As recoil. The threshold energies for the generation of defects in As cascades were 30, 40, and 120 eV for point defects, small clusters, and large clusters, respectively (Fig. 5).

The ratio of the number of vacancies to the number of interstitials in the WS defect analysis is shown in Table I.

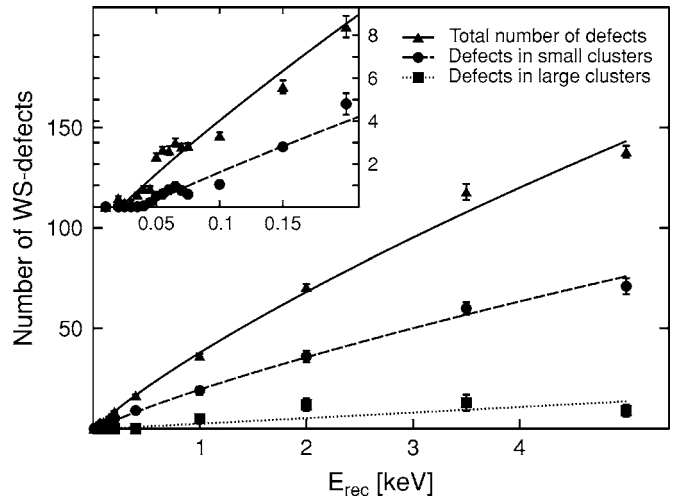


FIG. 5. WS defects produced by As recoils in GaAs₉₀N₁₀.

Point defects produced by As recoils in GaAs and GaAsN are more likely to be interstitials than vacancies, while the opposite is true for the N recoils in GaAsN.

Figure 6 shows a division of WS defects into various types of clusters for the case of N recoil cascades. No more than 14 defects exist in the same cluster. The threshold energies are slightly higher than those in the As-recoil simulations, namely, 40, 65, and 450 eV for the point defects, small, and large clusters, respectively. It is worth noting that only a small fraction of defects are in large clusters produced by N recoil cascades.

The defect type contents in small clusters show no dependency on the type of recoil atoms. At $E_{\text{rec}} = 400$ eV, vacancies are twice more abundant than interstitials in the clusters. This ratio levels off at higher energies and is about 1.4 at $E_{\text{rec}} = 10$ keV. In large clusters produced by N recoils, no interstitials can be found.

Antisites are produced by As recoils in GaAs, GaAsN, and N recoils in GaAsN at energies above a threshold energy of approximately 35, 20, and 30 eV, respectively. Similar to the case of other WS defects (vacancies and interstitials), the number of antisites exhibit an asymptotically linear behavior,

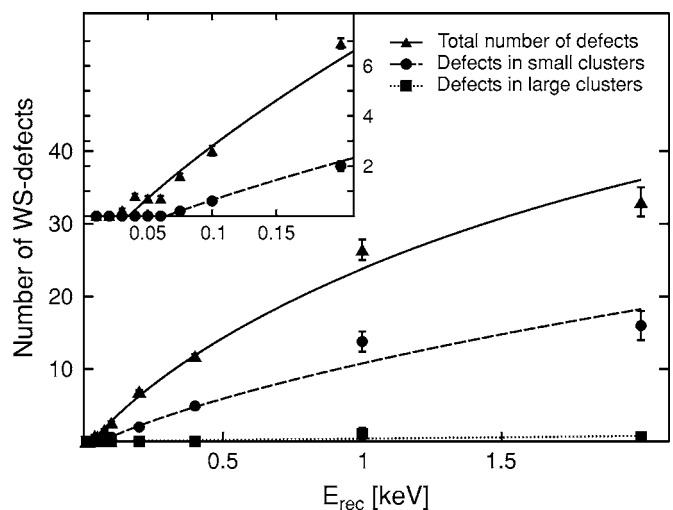


FIG. 6. WS defects produced by N recoils in GaAs₉₀N₁₀.

TABLE I. Ratio between vacancies (V) and interstitials (I) in GaAs and GaAs₉₀N₁₀. Small clusters contain between two and ten defects.

E_{rec} (keV)	0.4	1	2	5	10
<i>V/I</i> in point defects					
GaAs As recoil	0.43±0.05	0.44±0.05	0.43±0.02	0.33±0.06	0.44±0.03
GaAsN As recoil	0.38±0.04	0.40±0.05	0.39±0.04	0.42±0.04	
N recoil	0.58±0.05	0.54±0.08	0.57±0.08		
<i>V/I</i> in small clusters					
GaAs As recoil	2.6±0.4	1.7±0.2	1.7±0.2	1.55±0.11	1.44±0.13
GaAsN As recoil	2.3±0.3	1.1±0.2	1.22±0.13	1.59±0.15	
N recoil	2.3±0.4	1.4±0.3	1.7±0.2		
<i>V/I</i> in large clusters					
GaAs As recoil	...	no I	9±7	3.8±1.4	2.0±0.8
GaAsN As recoil	...	no I	4.1±0.2	no I	
N recoil	...	no I	no I		

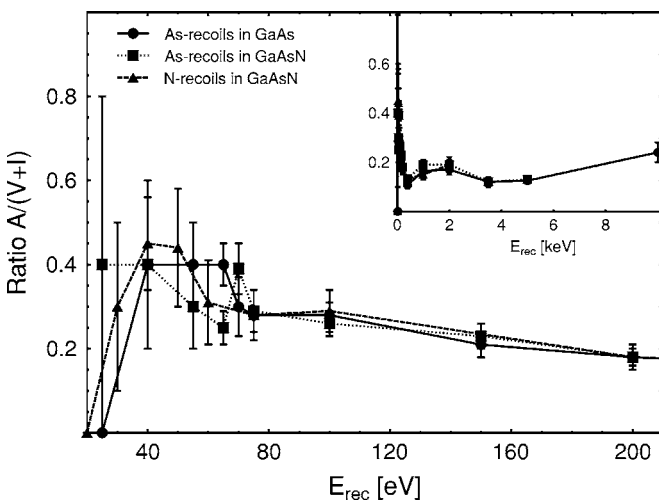
as E_{rec} is varied. Figure 7 compares the number of antisites with the number of vacancies and interstitials, showing that the antisites are produced in significant amounts at low recoil energies. Furthermore, it shows that antisites are also produced in GaAsN by N recoils and that the number of these antisites compared to the other two defect types is similar to the ratio in As recoils.

The proportion of Ga in interstitials in GaAs is shown in Table II. About 60% of the defects are Ga interstitials in GaAs, due to the lower formation energy of Ga interstitial compared to an As interstitial in GaAs.²⁶

The distribution of interstitials in GaAsN (see Table III) indicates that 30% are As interstitials, 60% are Ga interstitials (the same as for GaAs), and the remaining 10% are N interstitials (at high E_{rec}).

Figure 8 illustrates clusters of different sizes. (a) shows small clusters of each WS defect, and (b), on the other hand, shows large clusters of each WS defect. A few point defects are seen, as well.

We also studied the question, to what extent the defects remain in GaAsN upon heat treatment. Therefore, we heated the cells damaged by As recoils up to 1000 K and then

FIG. 7. Ratio between antisites (A) and vacancies (V) and interstitials (I).

quenched the cells to 0 K in 10 ps. The amount of damage was remarkably reduced. In particular, no large pockets survived this procedure, and only a very few point defects remained.

C. Total damage production

Evaluation of the integral in Eq. (1) gives an estimate of the total damage produced in GaAs and GaAsN. The results are given in Table IV and illustrated in Fig. 9.

There is a remarkable difference in damage production between the two irradiation directions (0° and 7°). N_{tot} created at 0° is only 5%–10% of the damage made by irradiation at 7° . In large clusters, damage depended also on the type of the incoming ion. When GaAs was irradiated (at 7°) with Ni, 17% of damage was in clusters with more than ten defects (large clusters), but when GaAs was irradiated with H ions, less than 3% of damage was in large clusters.

The studies on GaAsN revealed the same overall tendency of defects to be ion specific. At high recoil energies, the number of large clusters increased, though not as dramatically as in the case of GaAs; the largest amount of damage was 9%, obtained for Ni irradiation. Comparing GaAs and GaAsN, the different irradiation ions produced practically the same total amount of damage per ion in GaAs as in GaAsN (see last column in Table IV). The damage is distributed differently into point defects versus defect clusters, however. In GaAsN a smaller fraction of the damage is in large clusters.

IV. DISCUSSION

Figures 4–6 clearly show that a major fraction of the primary damage induced by self-recoils in GaAs and GaAsN is in clusters, for all recoil energies above roughly 100 eV.

TABLE II. Fraction of gallium atoms in WS interstitials in GaAs. Defects were produced by As self-recoils.

E_{rec} (keV)	0.4	1	2	5	10
Ga/Tot (%)	59.3±0.2	61.3±0.5	60.76±0.05	60.33±0.05	59.7±0.3

TABLE III. Atom-type distribution in WS interstitials in GaAs₉₀N₁₀. The values are given in percent of the total amount of interstitials.

E_{rec} (keV)	0.4	1	2	5
GaAsN As recoil				
Ga/Tot	59.34±0.08	61.9±0.2	62.23±0.06	61.76±0.07
As/Tot	35.06±0.04	31.43±0.08	28.57±0.04	28.50±0.02
N/Tot	5.31±0.01	6.676±0.012	9.19±0.01	9.74±0.01
GaAsN N recoil				
Ga/Tot	58.1±0.2	59.29±0.12	60.4±0.4	61.9±0.8
As/Tot	27.03±0.09	33.28±0.08	29.5±0.2	30.0±0.3
N/Tot	14.83±0.03	7.432±0.014	10.04±0.02	8.10±0.03

For instance, even at the relatively low energy of 400 eV about half of the damage in both GaAs and GaAsN is in (small or large) clusters, both for As and N recoils. However, the As recoils tend to produce more large clusters than N recoils do. These large clusters are strongly disordered (amorphous) and vacancy rich. These results are in line with other simulations and experiments on ion-irradiated damages in elemental and binary semiconductors.^{16,18,31–33} The experiments have also shown that in GaAs amorphous pockets recrystallize at room temperature.¹² While this effect is not included in our simulations, it does not change the fact that the differences in heavy ion damage normalized by deposited energy must be reflected in the primary damage.

Relatively low threshold energies of 20–35 eV needed to form antisites is consistent with earlier reports,^{34,35} suggesting that antisites can be formed directly by single atom recoils in GaAs. Our simulations further indicated that the direct formation of As antisites is possible also by N recoils, which is not an obvious result since the low mass of N makes it more difficult for it to displace a heavier As from a lattice site. Moreover, for N recoils the fraction of N antisites compared to Ga and As ones is quite high, up to about 0.5 for the energies below 100 eV.

The fraction of damage in antisites of any type is also high, between 0.1 and 0.3 at all E_{rec} . This is important since antisites at least in pure GaAs are quite stable, requiring high temperatures to anneal out.³⁶ In a previous work we have shown that antisites persist also after annealing of an amorphous zone.¹⁸ This, in combination with the observation that the amorphous zones are vacancy rich, indicates that even

though the amorphous zones (at least in GaAs) anneal even at room temperature, a sizable fraction of the damage in them will remain in the form of vacancies and/or antisites.

The formation energy of an N interstitial in GaN is not much lower than the formation energy of a Ga one.³⁷ Hence, our observation that there are about twice as many N interstitials than the stoichiometry would warrant, must be related to the low mass of N atoms, making interstitial formation easy in the ballistic phase of the cascade.

We now proceed to explore N_{tot} produced by incoming ions. The results that are presented in Table IV and illustrated in Fig. 9 show that the fraction of damage in small and large clusters is significant even by H irradiation at $E_{\text{ion}} = 100$ keV, corresponding to about 40% of all damage in GaAs and 50% in GaAsN. This fraction increases with the ion mass, being about 60% for 10 MeV Ni for both GaAs and GaAsN. It is interesting to note that the fraction of damage does not change much with ion mass. The fraction of damage in large clusters (more than ten WS defects or more than about 70 atoms) does increase strongly with mass, however. This fraction is 2%–4% for H, 6%–8% for He, 8%–14% for Ne, and 9%–17% for Ni. The fact that Ne produces almost as much damage in large clusters as Ni does is somewhat surprising considering that Ne is about three times lighter than Ni.

Although our criterion for defining a “large” cluster is of course somewhat arbitrary, the same qualitative conclusions would be reached also for other limits. Using an even higher threshold to define a “very large” cluster (50 Wigner-Seitz defects) showed that no very large clusters were formed for H irradiation, while some did form for the Ni irradiations. This observation is well in line with transmission electron microscopy (TEM) experiments,⁸ which show that proton irradiations did not produce any defects visible in the TEM, while Ni irradiations did.

Our results indicate that differences in carrier dynamics, due to ion irradiation by various ion species having the same nuclear deposited energy, are related to the types of defects generated. The defects can be attributed to the existence of large clusters either in the form of amorphous zones or clustered vacancies and antisites, which persist in the samples after the zones have recrystallized. Therefore, we suggest that the carrier decay time decreases with an increasing fraction of damage particularly in large clusters.

In the light of a recent report¹³ on thermal stability of Ni-induced damage in InGaAs, it appears that the carrier lifetime depends on an aging process. A twofold increase in lifetime was obtained in all Ni irradiated samples when the measurements were made after 45 days of aging at room temperature. On the other hand, rapid thermal annealing (RTA) at 610 °C for 1 s gave rise to quick lattice recovery and, consequently, much longer lifetimes. This effect can be interpreted by the present calculations. Ni irradiation produces large amorphous defect clusters, which, however, can be removed by maintaining the sample at room temperature for a long time,¹² or even more effectively, by annealing at high temperature where the defects with high threshold energies, including most of the point defects, are removed.

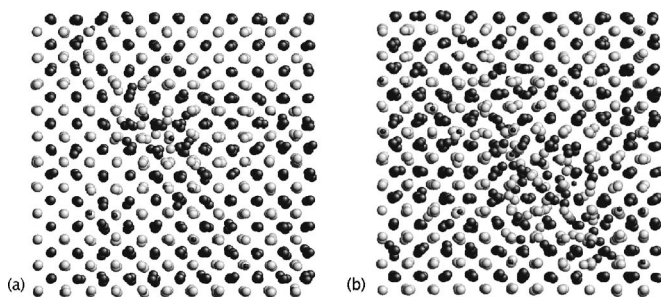


FIG. 8. Typical distributions of damage in GaAs₉₀N₁₀ produced in cascade simulations. (a) shows damage in two small clusters; one vacancy and one interstitial cluster. The damage in (b) is in large clusters. The small black spheres represent nitrogen atoms, the big black spheres arsenide atoms, and the gray spheres gallium atoms.

TABLE IV. Total damage production in GaAs and GaAs₉₀N₁₀ between the depths of 80 and 200 nm. Small clusters are defect clusters containing two to ten Wigner-Seitz defects. The angle indicates the irradiation direction and is measured in degrees off the [100] crystal direction.

Recoil ion	Substrate	Angle	Damage in small clusters	Damage in large clusters	Total damage/ion
$E_{\text{ion}}=100$ keV	GaAs	7°	0.613±0.005	0.0408±0.0004	1.606±0.002
		0°	0.0290±0.0002	0.00178±0.00002	0.0767±0.0001
	GaAs ₉₀ N ₁₀	7°	0.676±0.006	0.063±0.003	1.536±0.006
		0°	0.0294±0.0007	0.0006±0.0003	0.1247±0.0007
$E_{\text{ion}}=200$ keV	GaAs	7°	5.65±0.03	1.05±0.04	13.87±0.04
		0°	0.260±0.003	0.0396±0.0014	0.642±0.004
	GaAs ₉₀ N ₁₀	7°	6.50±0.10	0.81±0.09	13.71±0.08
		0°	0.309±0.007	0.033±0.004	0.672±0.006
$E_{\text{ion}}=400$ keV	GaAs	7°	251±5	84±4	584±3
		0°	20.4±0.4	6.2±0.3	48.9±0.2
	GaAs ₉₀ N ₁₀	7°	290±6	45±7	568±5
		0°	29.4±0.6	4.3±0.6	58.8±0.5
$E_{\text{ion}}=10$ MeV	GaAs	7°	284±8	113±6	664±4
		0°	19.7±0.2	4.7±0.2	46.6±0.2
	GaAs ₉₀ N ₁₀	7°	347±8	57±9	666±6
		0°	26.6±0.6	3.8±0.6	53.5±0.5

V. CONCLUSIONS

We have studied the damage production by high-energy (100 keV–10 MeV) H, He, Ne, and Ni ions in GaAs and GaAs₉₀N₁₀ using molecular dynamics computer simulations. We find that the heavier Ne and Ni ions produce a larger fraction of damage in large clusters. These are either in the form of amorphous zones or (after room-temperature aging or high-temperature annealing) in the form of vacancy and antisite clusters. The total damage production in GaAs and GaAs₉₀N₁₀ is the same for all the ions; however, a clearly smaller fraction of the damage in GaAs₉₀N₁₀ is in large clusters compared to GaAs. Our results indicate that experimentally observed differences in charge carrier lifetimes between light and heavy ion irradiations, and before and after annealing, can be understood in terms of the large defect clusters. An increasing amount of damage in large clusters decreases the carrier decay time.

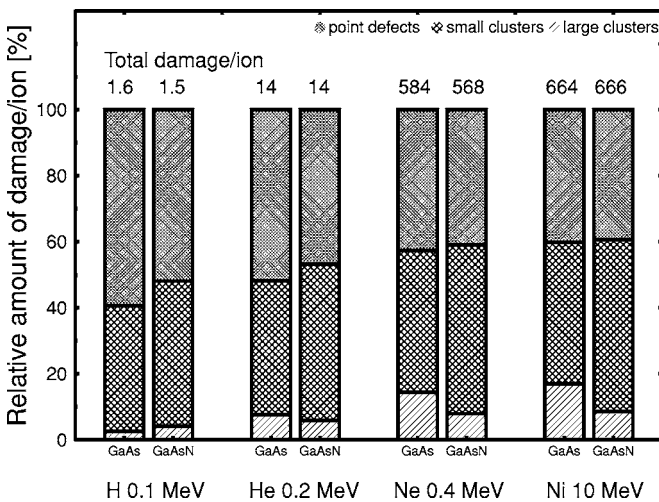


FIG. 9. Final defect distribution of the implantation.

ACKNOWLEDGMENTS

This research was funded by the QUEST research consortium, Academy of Finland research Project No. 202718. Grants of computer time from the Center for Scientific Computing in Espoo, Finland and the M-GRID cluster computing network are gratefully acknowledged.

- ¹B. Gil, *Low Dimensional Nitride Semiconductors* (Oxford University Press, Oxford, 2002).
- ²O. Okhotnikov and M. Pessa, *J. Phys.: Condens. Matter* **16**, S3107 (2004).
- ³O. Okhotnikov, A. Grudin, and M. Pessa, *New J. Phys.* **6**, 177 (2004).
- ⁴C. W. Coldren, M. C. Larson, S. G. Spruytte, and J. S. Harris, Jr., *Electron. Lett.* **36**, 951 (2000).
- ⁵M. R. Gokhale, P. V. Studenkov, J. Wei, and S. R. Forrest, *IEEE Photonics Technol. Lett.* **12**, 131 (2000).
- ⁶C. S. Peng, T. Jouhti, P. Laukkanen, E.-M. Pavelescu, J. Kontinen, W. Li, and M. Pessa, *IEEE Photonics Technol. Lett.* **14**, 275 (2002).
- ⁷T. Hakkarainen *et al.*, *J. Phys. D* **38**, 985 (2005).
- ⁸J. Mangeney, H. Chouman, G. Patriarche, G. Leroux, G. Aubi, J. Harmand, J. L. Oudar, and H. Bernas, *Appl. Phys. Lett.* **79**, 2722 (2001).
- ⁹L. Joulaud, J. Mangeney, J.-M. Lourtioz, P. Crozat, and G. Patriarche, *Appl. Phys. Lett.* **82**, 856 (2003).
- ¹⁰E. Lugagne Delpon, J. Oudar, N. Bouché, R. Raj, A. Shen, N. Stehlakh, and J. Lourtioz, *Appl. Phys. Lett.* **72**, 759 (1998).
- ¹¹V. D. S. Dhaka, N. V. Tkachenko, H. Lemmetyinen, E.-M. Pavelescu, M. Guina, A. Tukiainen, J. Kontinen, M. Pessa, K. Arstila, J. Keinonen, and K. Nordlund, *Semicond. Sci. Technol.* **21**, 661 (2006).
- ¹²M. W. Bench, I. M. Robertson, M. A. Kirk, and I. Jenčić, *J. Appl. Phys.* **87**, 49 (2000).
- ¹³V. D. S. Dhaka, N. V. Tkachenko, H. Lemmetyinen, E.-M. Pavelescu, J. Kontinen, K. Arstila, and J. Keinonen, *Electron. Lett.* **41**, 23 (2005).
- ¹⁴V. D. S. Dhaka, N. V. Tkachenko, H. Lemmetyinen, E.-M. Pavelescu, S. Suomalainen, M. Pessa, K. Arstila, J. Keinonen, and K. Nordlund, *J. Phys. D* **39**, 2659 (2006).
- ¹⁵K. Nordlund and A. Kuronen, *Nucl. Instrum. Methods Phys. Res. B* **115**, 528 (1996).
- ¹⁶K. Nordlund, M. Ghaly, R. S. Averback, M. Caturla, T. Diaz de la Rubia, and J. Tarus, *Phys. Rev. B* **57**, 7556 (1998).
- ¹⁷K. Nordlund, L. Wei, Y. Zhong, and R. S. Averback, *Phys. Rev. B* **57**, R13965 (1998).
- ¹⁸K. Nordlund, J. Peltola, J. Nord, J. Keinonen, and R. S. Averback, *J. Appl. Phys.* **90**, 1710 (2001).

- ¹⁹S. O. Kucheyev, J. S. Williams, C. Jagadish, J. Zou, G. Li, and A. I. Titov, *Phys. Rev. B* **64**, 035202 (2001).
- ²⁰E. Wendler, A. Kamarou, E. Alves, K. Gärtner, and W. Wesch, *Nucl. Instrum. Methods Phys. Res. B* **206**, 1028 (2002).
- ²¹J. Nord, K. Nordlund, and J. Keinonen, *Phys. Rev. B* **68**, 184104 (2003).
- ²²K. Nordlund, J. Nord, J. Frantz, and J. Keinonen, *Comput. Mater. Sci.* **18**, 283 (2000).
- ²³K. Nordlund, *Comput. Mater. Sci.* **3**, 448 (1995).
- ²⁴J. F. Ziegler, J. P. Biersack, and U. Littmark, *The Stopping and Range of Ions in Matter* (Pergamon, New York, 1985).
- ²⁵J. F. Ziegler, SRIM-96, computer code, 1996; (private communication).
- ²⁶K. Albe, K. Nordlund, J. Nord, and A. Kuronen, *Phys. Rev. B* **66**, 035205 (2002).
- ²⁷K. Nordlund, PARCAS computer code. The main principles of the molecular dynamics algorithms are presented in Refs. 16 and 40. The adaptive time step and electronic stopping algorithms are the same as in Ref. 23.
- ²⁸M. P. Allen and D. J. Tildesley, *Computer Simulation of Liquids* (Oxford University Press, Oxford, England, 1989).
- ²⁹H. J. C. Berendsen, J. P. M. Postma, W. F. van Gunsteren, A. DiNola, and J. R. Haak, *J. Chem. Phys.* **81**, 3684 (1984).
- ³⁰Since the diamond/zinc blende crystal structure is not a Bravais lattice, the cells centered at the lattice atoms are strictly speaking Voronoi polyhedra. See, e.g., N. W. Ashcroft and N. D. Mermin, *Solid State Physics* (Saunders, Philadelphia, 1976), Chap. 4.
- ³¹T. Diaz de la Rubia, R. S. Averback, R. Benedek, and W. E. King, *Phys. Rev. Lett.* **59**, 1930 (1987); **60**, 76 (1988).
- ³²M. W. Bench, I. M. Robertson, and M. A. Kirk, *Nucl. Instrum. Methods Phys. Res. B* **59/60**, 372 (1991).
- ³³I. Jenčič, M. W. Bench, I. M. Robertson, and M. A. Kirk, *J. Appl. Phys.* **78**, 974 (1995).
- ³⁴T. Mattila and R. M. Nieminen, *Phys. Rev. Lett.* **74**, 2721 (1995).
- ³⁵H. Hausmann, A. Pillukat, and P. Ehrhart, *Phys. Rev. B* **54**, 8527 (1996).
- ³⁶S. Kuisma, K. Saarinen, P. Hautajarvi, and C. Corbel, *Phys. Rev. B* **55**, 9609 (1997).
- ³⁷J. Nord, K. Albe, P. Erhart, and K. Nordlund, *J. Phys.: Condens. Matter* **15**, 5649 (2003).
- ³⁸N. Tkachenko, L. Rantala, A. Y. Tauber, J. Helaja, P. H. Hynninen, and H. Lemmetyinen, *J. Am. Chem. Soc.* **21**, 9379 (1999).
- ³⁹J. F. Ziegler, SRIM-2003, software package (available online at <http://www.srim.org>).
- ⁴⁰M. Ghaly, K. Nordlund, and R. S. Averback, *Philos. Mag. A* **79**, 795 (1999).